Faraday Discuss. Chem. Soc., 1986, **82**, 327–342

Vibrational Predissociation of the Ethylene Dimer

Andrew C. Peet, David C. Clary and Jeremy M. Hutson*†

University Chemical Laboratory, Lensfield Road, Cambridge CB2 1EW

The energies, lifetimes and product state distributions for vibrational predissociation of the van der Waals complex $(C_2H_4)_2$ have been calculated. A coupled channel method, which includes both vibration and azimuthal rotation of the ethylene monomers, has been used. Lifetimes are found to be of the order of 10^{-6} s, which supports the recent observation by Snels *et al.* that fine structure exists within the infrared photodissociation spectrum. A curve-crossing mechanism proposed by Ewing is also investigated but cannot account for lifetimes on the picosecond timescale.

There has been much experimental interest over the last few years in the vibrational predissociation of van der Waals complexes.[1] In the experiments usually carried out, one of the constituent molecules is vibrationally excited using an infrared laser source and if the energy gained is greater than the binding energy of the van der Waals bond the complex dissociates. The finite lifetime which results from such predissociation leads to a broadening of the lines in the infrared spectrum.

Experiments carried out on complexes involving linear molecules, such as $(C_2H_2)_2$,[2] $(CO_2)_2$[3] and $(HF)_2$,[4] generally show infrared spectra consisting of narrow lines, giving a lower limit to the lifetimes of such complexes of the order of 10^{-9} s. Sharp spectra have also been observed for the dimer of the symmetric top molecule methylacetylene;[2] in this case the lower limit to the lifetime is 5×10^{-8} s. In contrast to these results, the photodissociation specta of van der Waals complexes involving most other polyatomic molecules have been observed to be broad and featureless,[1] with lines up to several tens of wavenumbers wide. It was originally supposed that these spectra were homogeneously broadened and that the lifetimes of the complexes were of the order of 10^{-12} s.

For complexes containing polyatomic molecules there are many rotational states present, arising from both rotation of the complex as a whole and hindered internal rotation of the monomers. If a broad featureless spectrum is observed, it may be due either to homogeneous broadening associated with a very short lifetime or to spectral congestion resulting from the overlap of a large number of relatively narrow lines. Such spectral congestion becomes more likely as the symmetry of the monomer decreases and will be particularly severe for complexes containing asymmetric tops.

The polyatomic systems which have been most extensively studied are the ethylene-containing clusters.[5–12] Early experiments on such clusters showed broad, essentially Lorentzian lines with widths between 1.6 and 17.5 cm^{-1}. More recently, structure has been observed in the spectra of some ethylene complexes. For example, Western *et al.*[5] observed structure in the spectra of Ne–C_2H_4 and Ar–C_2H_4; however, the lines seen were still broad compared with those seen in the spectra of complexes containing linear molecules, and lower bounds to the lifetimes of 10^{-11} s for Ne–C_2H_4 and 1.7×10^{-12} s for Ar–C_2H_4 were proposed.

The ethylene dimer has been the subject of particularly extensive study.[6–12] Until very recently all measurements of its spectrum showed a single Lorentzian line *ca.* 10 cm^{-1} wide, suggesting a lifetime of *ca.* 10^{-12} s. Since the complex is formed from two asymmetric top molecules it is expected that the spectrum will consist of a great number of lines and it is not immediatey clear whether each of the constituent lines is broadened to 10 cm^{-1} or whether a great number of much narrower lines overlap to

† Present address: Department of Chemistry, University of Durham, Science Laboratories, South Road, Durham DH1 3LE.

form a broad envelope. In an attempt to resolve this ambiguity, Mitchell *et al.*[9] carried out a direct time-domain experiment and found that >90% of their clusters were dissociated within a time of 10 ns from excitation. This upper limit to the lifetime gives a lower limit to the linewidth of 10^{-4} cm^{-1}, although the lines might be much broader than this.

Most of the experiments performed to date have used a mass spectrometer to measure the fraction of dimers dissociated by the laser. The $(C_2H_4)_2^+$ peak is monitored and its modulation by the laser is related to the fraction of dimers dissociated. Unfortunately, such experiments do not discriminate effectively between dimers and higher polymers. If trimers and larger clusters are present, they may be dissociated by either laser excitation or electron impact to yield $(C_2H_4)_2$, leading to a false increase in the signal. Hence, it is possible that contributions from higher polymers make a significant contribution to the observed spectra. To test this, Huisken *et al.*[10] crossed the cluster-containing beam with a beam of He atoms. The deflection caused by the collision of the cluster with an He atom depends upon the mass of the cluster, so that the method is capable of selecting specific polymers. Results from these experiments show that beams containing ethylene may actually be dominated by higher polymers rather than dimers.[11] This fact should always be remembered when discussing experiments where mass-spectrometric detection is employed, and casts some doubt on whether some of the experimental results really refer to the dimer.

Very recently, Snels *et al.*[12] have carried out experiments which show two types of structure in the ethylene dimer spectrum in the range 900–1000 cm^{-1}. First, they have found three Lorentzian lines separated by *ca.* 40 cm^{-1}, with the central one being close to the frequency (949 cm^{-1}) of the monomer vibration (ν_7) excited. The other two (much weaker) peaks they assign to simultaneous excitation (or de-excitation) of van der Waals mode. Secondly, and more importantly, they have found fine structure within the broad bands by tuning across individual CO_2 laser lines. This structure has a width of *ca.* 10^{-4} cm^{-1} and gives a lower limit for the lifetime of 16 ns.

It is clear that there is still much which is not understood in the photodissociation spectra of van der Waals molecules in general and the ethylene dimer in particular. In view of the uncertainties in the experimental results, this is a subject where theoretical work can make a valuable contribution. There have been many realistic theoretical studies of vibrational predissociation in atom–diatom complexes,[13–16] and a smaller number of such calculations on diatomic dimers.[17] For van der Waals complexes involving polyatomic molecules, however, very few theoretical computations of any quality have been performed. Most of the existing calculations have involved very drastic dynamical approximations. This is largely because scattering calculations involving polyatomic molecules are very expensive to perform and because there is little information available on the potential-energy surfaces for such systems.

The calculations on atom–diatom systems have shown that it is important to include coupling between rotational and vibrational motions in coupled channel calculations on vibrational predissociation. This has been done previously for vibrational predissociation of Ne–C_2H_4 and Ar–C_2H_4,[18] using a sudden approximation[19] specially adapted for atom–symmetric top collisions. In this paper we extend the atom–symmetric top approximation to symmetric top–symmetric top systems and apply it to the vibrational predissociation of the ethylene dimer. We calculate linewidths, lifetimes and product state distributions into the ethylene monomer rotational states which are energetically accessible. We compare our results with the experimental data and also with results obtained from more approximate theories.

Theory

The calculations are performed using the azimuthal and vibrational close-coupled, rotational infinite order sudden (AVCC-IOS) method.[19] The theory has been described

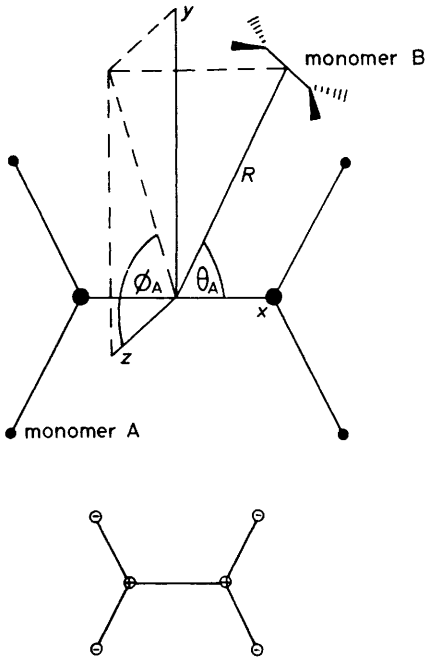

Fig. 1. Molecule-fixed coordinate system for monomer A. Two of the angles (θ_A and ϕ_A) which specify the relative orientation of the two monomers are shown. The lower part of the figure shows the nuclear displacements for the ν_7 mode of ethylene.

previously for both scattering[19] and vibrational predissociation[18] of atom-prolate symmetric top systems. Here, we extend the theory to the vibrational predissociation of a prolate symmetric top–prolate symmetric top complex. The method is described for the ethylene dimer, but its extension to other systems is straightforward.

Ethylene is a prolate near-symmetric top, with rotational constants $a = 4.72\ \mathrm{cm}^{-1}$, $b = 1.00\ \mathrm{cm}^{-1}$ and $c = 0.82\ \mathrm{cm}^{-1}$. Its vibration-rotation Hamiltonian may be approximated in normal mode-symmetric top form

$$h_A = \sum_i \left(-\frac{\hbar^2}{2}\frac{d^2}{dq_{Ai}^2} + \tfrac{1}{2}k_{Ai}q_{Ai}^2 \right) + (a-\bar{b})j_{xA}^2 + \bar{b}j_A^2, \tag{1}$$

where $\bar{b} = \frac{1}{2}(b+c)$, the subscript A identifies the monomer concerned, and all other quantities are standard. The molecular axis system is given in fig. 1 and follows the convention of Herzberg.[20] Note that the x axis lies along the C—C bond.

A body-fixed (BF) axis system is used, with the z axis along the vector joining the centres of mass of the two molecules. The orientations of the monomers are specified relative to this BF system[21] by Euler angles[22] (ξ_A, θ_A, ϕ_A) and (ξ_B, θ_B, ϕ_B) for monomers A and B, respectively. The angles θ_A and θ_B are the polar angles between the intermolecular vector and the C—C axes of the ethylene molecules, and ϕ_A and ϕ_B are the azimuthal angles for rotation of the monomers about the C—C bonds. The fifth angle required to specify the relative orientation of the monomers is the torsional angle between the C—C axes, $\xi = \xi_A - \xi_B$.

The Hamiltonian of the van der Waals complex may be written in this body-fixed axis system as

$$\mathscr{H} = \frac{\hbar^2}{2\mu}\left(-R^{-1}\frac{d^2}{dR^2}R + \frac{(\boldsymbol{J}-\boldsymbol{j}_A-\boldsymbol{j}_B)^2}{R^2} \right) + h_A + h_B + V_I(R, \theta_A, \phi_A, \theta_B, \phi_B, \xi, \boldsymbol{q}_A, \boldsymbol{q}_B) \tag{2}$$

where μ is the collisional reduced mass, $\boldsymbol{J}$ is the total angular momentum operator for the complex and $V_I(R, \theta_A, \phi_A, \theta_B, \phi_B, \xi, \boldsymbol{q}_A, \boldsymbol{q}_B)$ is the intermolecular potential, which is a function of the angular variables, the intermolecular distance R and the set of ethylene normal mode coordinates on the two monomers $\boldsymbol{q}_A$ and $\boldsymbol{q}_B$.

In order to make the problem tractable we now apply the helicity decoupling approximation in which the operator $(\boldsymbol{J}-\boldsymbol{j}_A-\boldsymbol{j}_B)^2$ is replaced by $[J(J+1)-2\Omega^2]+(\boldsymbol{j}_A+\boldsymbol{j}_B)^2$. The resulting Schrödinger equation is still computationally intractable, but further simplification is possible because the ethylene rotational constant $\bar{b}=0.91\ \mathrm{cm}^{-1}$ is much smaller than the rotational constant describing rotation about the C—C axis, $(a-\bar{b})=3.81\ \mathrm{cm}^{-1}$. The van der Waals bending motions, described by the angles θ_A, θ_B and ξ, are slower than the van der Waals stretching (R) and azimuthal rotations (ϕ_A, ϕ_B). This allows the bending angle-dependent part of the wavefunction to be approximately factorised out. The wavefunction is written in the form

$$\Psi = R^{-1}\psi(R, \phi_A, \phi_B, \boldsymbol{q}_A, \boldsymbol{q}_B; \theta_A, \theta_B, \xi)\Theta(\theta_A, \theta_B, \xi) \tag{3}$$

where $\psi(R, \phi_A, \phi_B, \boldsymbol{q}_A, \boldsymbol{q}_B; \theta_A, \theta_B, \xi)$ depends only parametrically upon the bending angles θ_A, θ_B and ξ and is a solution of the equation

$$\left(-\frac{\hbar^2}{2\mu}\frac{\mathrm{d}^2}{\mathrm{d}R^2}+\bar{h}_A+\bar{h}_B+V_I(R, \theta_A, \phi_A, \theta_B, \phi_B, \xi, \boldsymbol{q}_A, \boldsymbol{q}_B)-E\right)$$
$$\times\psi(R, \phi_A, \phi_B, \boldsymbol{q}_A, \boldsymbol{q}_B; \theta_A, \theta_B, \xi)=0. \tag{4}$$

$\bar{h}_A$ and $\bar{h}_B$ are the molecular hamiltonians with the operators $\boldsymbol{j}_A^2$ and $\boldsymbol{j}_B^2$ neglected. Below the lowest dissociation limit, eqn (4) is an eigenvalue equation and the locus of the eigenvalues $E_m(\theta_A, \theta_B, \xi)$ forms an effective bending potential. Even at energies in the continuum, the equation is effectively an eigenvalue equation if the energy is close to a predissociating state, so that an upper-state bending potential can also be defined. Substitution of the wavefunction Ψ of eqn (3) into the helicity decoupled Schrödinger equation yields the equation

$$\left(E-E_m(\theta_A, \theta_B, \xi)-\bar{b}(\boldsymbol{j}_A^2+\boldsymbol{j}_B^2)-\frac{\hbar^2}{\mu R^2}[J(J+1)-2\Omega^2+(\boldsymbol{j}_A+\boldsymbol{j}_B)^2]\right)$$
$$\times\psi(R, \phi_A, \phi_B, \boldsymbol{q}_A, \boldsymbol{q}_B; \theta_A, \theta_B, \xi)\Theta(\theta_A, \theta_B, \xi)=0. \tag{5}$$

This equation is simplified by making the angular adiabatic approximation:

$$(\boldsymbol{j}_A^2+\boldsymbol{j}_B^2)\psi(R, \phi_A, \phi_B, \boldsymbol{q}_A, \boldsymbol{q}_B; \theta_A, \theta_B, \xi)\Theta(\theta_A, \theta_B, \xi)$$
$$=\psi(R, \phi_A, \phi_B, \boldsymbol{q}_A, \boldsymbol{q}_B; \theta_A, \theta_B, \xi)(\boldsymbol{j}_A^2+\boldsymbol{j}_B^2)\Theta(\theta_A, \theta_B, \xi) \tag{6}$$

which assumes that ψ varies only slowly with the bending angles θ_A, θ_B and ξ. Multiplying on the left by $\psi^*(R, \phi_A, \phi_B, \boldsymbol{q}_A, \boldsymbol{q}_B; \theta_A, \theta_B, \xi)$ and integrating over R, ϕ_A, ϕ_B, $\boldsymbol{q}_A$ and $\boldsymbol{q}_B$ gives

$$\{E-E_m(\theta_A, \theta_B, \xi)-\bar{b}(\boldsymbol{j}_A^2+\boldsymbol{j}_B^2)-B_e[J(J+1)-2\Omega^2+(\boldsymbol{j}_A+\boldsymbol{j}_B)^2]\}\Theta(\theta_A, \theta_B, \xi)=0 \tag{7}$$

where B_e is an effective rotational constant for the complex and is the expectation value of R^{-2} over the wavefunction $\psi(R, \phi_A, \phi_B, \boldsymbol{q}_A, \boldsymbol{q}_B; \theta_A, \theta_B, \xi)$. An explicit expression for B_e is given in eqn (10) below. Eqn (7) is just a hindered rotor problem involving the bending potential $E_m(\theta_A, \theta_B, \xi)$, and its solution yields the energy levels of the bound complex and energies of predissociating states. The main part of the problem thus reduces to solving the fixed-angle stretching equation (4), and the remainder of the present paper will concentrate on this.

Calculation of Spectral Linewidths

Spectral linewidths are identified with the widths of resonant features in the continuum solutions of eqn (4). This equation is solved by expanding the fixed-angle wavefunction $\psi(R, \phi_A, \phi_B, \boldsymbol{q}_A, \boldsymbol{q}_B; \theta_A, \theta_B, \xi)$ in a close-coupled basis set of ethylene vibrational functions $\psi_{v_A}(\boldsymbol{q}_A)$ and $\psi_{v_B}(\boldsymbol{q}_B)$ and azimuthal functions $e^{ik_A\phi_A}$ and $e^{ik_B\phi_B}$. Thus the fixed-angle wavefunction is expanded as

$$\psi(R, \phi_A, \phi_B, \boldsymbol{q}_A, \boldsymbol{q}_B; \theta_A, \theta_B, \xi) = \sum_{v_A k_A v_B k_B} \Phi_{v_A k_A v_B k_B}(\boldsymbol{q}_A, \phi_A, \boldsymbol{q}_B, \phi_B) f_{v_A k_A v_B k_B}(R; \theta_A, \theta_B, \xi) \tag{8}$$

where

$$\Phi_{v_A k_A v_B k_B}(\boldsymbol{q}_A, \phi_A, \boldsymbol{q}_B, \phi_B) = \psi_{v_A}(\boldsymbol{q}_A) \exp(ik_A\phi_A)\psi_{v_B}(\boldsymbol{q}_B) \exp(ik_B\phi_B) \tag{9}$$

v_A and v_B represent sets of vibrational quantum numbers, and k_A and k_B represent azimuthal rotational quantum numbers for molecules A and B, respectively. With the wavefunction expanded in this manner, B_e of eqn (7) takes the form

$$B_e = \frac{\hbar^2}{2\mu} \sum_{v_A k_A v_B k_B} \int_0^\infty f_{v_A k_A v_B k_B} R^{-2} f_{v_A k_A v_B k_B} \, dR. \tag{10}$$

Substituting the wavefunction expansion of eqn (8) into eqn (4) yields the AVCC–IOS equations for the problem:

$$\left(\frac{d^2}{dR^2} + k^2_{v'_A k'_A v'_B k'_B}\right) f_{v'_A k'_A v'_B k'_B}(R; \theta_A, \theta_B, \xi) = \frac{2\mu}{\hbar^2} \sum_{v''_A k''_A v''_B k''_B} V^{v''_A k''_A v''_B k''_B}_{v'_A k'_A v'_B k'_B}(R; \theta_A, \theta_B, \xi) f_{v''_A k''_A v''_B k''_B}(R; \theta_A, \theta_B, \xi), \tag{11}$$

where

$$k^2_{v'_A k'_A v'_B k'_B} = \frac{2\mu}{\hbar^2}(E - E_{v'_A} - E_{k'_A} - E_{v'_B} - E_{k'_B}) \tag{12}$$

and the potential matrix elements are

$$V^{v''_A k''_A v''_B k''_B}_{v'_A k'_A v'_B k'_B}(R; \theta_A, \theta_B, \xi) = \int d\boldsymbol{q}_A \int d\boldsymbol{q}_B \int_0^{2\pi} d\phi_A \int_0^{2\pi} d\phi_B \Phi^*_{v'_A k'_A v'_B k'_B}(\boldsymbol{q}_A, \phi_A, \boldsymbol{q}_B, \phi_B) \times V_I(R, \theta_A, \phi_A, \theta_B, \phi_B, \xi, \boldsymbol{q}_A, \boldsymbol{q}_B) \times \Phi_{v''_A k''_A v''_B k''_B}(\boldsymbol{q}_A, \phi_A, \boldsymbol{q}_B, \phi_B). \tag{13}$$

The AVCC-IOS equations (11) are solved subject to scattering boundary conditions[19] to yield an S matrix which is dependent upon the fixed angles θ_A, θ_B and ξ. Predissociating states appear as resonant features in the energy dependence of the S-matrix elements. In the vicinity of a resonance, the eigenphase sum[23] increases sharply by π and the individual S matrix elements describe circles in the complex plane. Resonance energies $E_m(\theta_A, \theta_B, \xi)$ and widths $\Gamma_m(\theta_A, \theta_B, \xi)$ are obtained by fitting a Breit–Wigner function to the eigenphase sum and may be interpreted as energies and widths of predissociating states at particular values of θ_A, θ_B and ξ. To obtain the full predissociation energies and widths these should then be averaged over the bending wavefunctions of eqn (7). However, it is not practical to solve the AVCC-IOS equations for all values of the bending angles and so in the present work we only carry out the calculations at values of the fixed angles for which the bending wavefunction is largest. The lifetimes of the

predissociating states may be obtained from the widths by using the Heisenberg uncertainty relation:

$$\tau_m = \frac{\hbar}{\Gamma_m}. \tag{14}$$

Partial widths $\Gamma_{m v_A k_A v_B k_B}$ are obtained by fitting the diagonal S-matrix elements and give the product state distribution on predissociation.[23]

Computational Aspects

Even using the dynamical approximation of the last section, the computer time required to solve the coupled equations (11) as they appear there would be too large for the problem to be tractable. Here we present two aspects of the problem which allow the calculation to be carried out.

Symmetry

The intermolecular potential is totally symmetric with respect to the symmetry operations of both ethylene molecules. Thus, it is useful to solve the coupled equations (11) using a basis set of vibrational–rotational monomer wavefunctions which transform as irreducible representations of the ethylene point group D_{2h}. These monomer wavefunctions contain symmetrised azimuthal functions which are linear combinations of $\{\exp ik\phi\}$ and are of the form $\sin k\phi$ and $\cos k\phi$. The basis set $\{\Phi^{\Gamma_A \Gamma_B}_{v_A k_A v_B k_B}\}$ which is used in the expansion of eqn (8) is now a product of the symmetrised functions on the two monomers and is labelled by the symmetries of the vibration–rotation wavefunctions on the two monomers Γ_A and Γ_B. In this basis set, the potential matrix elements of eqn (11) are non-zero only between molecular wavefunctions of the same symmetry for each monomer and thus the AVCC–IOS equations can be solved using smaller basis sets. We use the notation Γ_A/Γ_B to indicate that the wavefunction of monomer A has symmetry Γ_A and the wavefunction of monomer B has symmetry Γ_B. More details of symmetry considerations are given in ref. (18).

If the fixed angles θ_A, θ_B and ξ are such that the complex has a centre of inversion, and the two monomer wavefunctions have the same total symmetry ($\Gamma = \Gamma_A = \Gamma_B$), a further simplification occurs. In this case the molecular product basis set can be symmetrised and

$$\Phi^{\Gamma\pm}_{v_A k_A v_B k_B}(\boldsymbol{q}_A, \phi_A, \boldsymbol{q}_B, \phi_B) = \sqrt{\tfrac{1}{2}}[\Phi^{\Gamma\Gamma}_{v_A k_A v_B k_B}(\boldsymbol{q}_A, \phi_A, \boldsymbol{q}_B, \phi_B) \pm \Phi^{\Gamma\Gamma}_{v_B k_B v_A k_A}(\boldsymbol{q}_A, \phi_A, \boldsymbol{q}_B, \phi_B)]. \tag{15}$$

This effects a two-fold reduction in basis-set size as the symmetrized and antisymmetrized basis functions are not coupled by the intermolecular potential.

Evaluation of the Potential Matrix Elements

The potential matrix elements of eqn (13) are evaluated in two stages. First, a direct quadrature is carried out over the vibrational motion of both monomers. This gives the vibrational potential matrix elements

$$V^{v'}_{v}(\phi_A, \phi_B, R) = \int \mathrm{d}\boldsymbol{q}_A \int \mathrm{d}\boldsymbol{q}_B \psi_{v_A}(\boldsymbol{q}_A)\psi_{v_B}(\boldsymbol{q}_B) V_I(R, \theta_A, \phi_A, \theta_B, \phi_B, \boldsymbol{q}_A, \boldsymbol{q}_B) \times \psi_{v'_B}(\boldsymbol{q}_A)\psi_{v'_B}(\boldsymbol{q}_B) \tag{16}$$

where v and v' are collective indices representing $v_A v_B$ and $v'_A v'_B$, respectively. The integration should, in principle, be carried out over all normal modes of both ethylene

Table 1. Symmetries of the functions used to expand the vibrational potential matrix elements under D_{2h}

function	k	symmetry
$\sin k\phi$	even	B_{3g} or A_u
$\sin k\phi$	odd	B_{1g} or B_{2u}
$\cos k\phi$	even	A_g or B_{3u}
$\cos k\phi$	odd	B_{2g} or B_{1u}

monomers; however, such a quadrature would be prohibitively expensive, so all the ethylene normal coordinates except those for ν_7 were set to their equilibrium values of zero. In the present work, the vibrational wavefunctions are harmonic oscillator functions and the integrals are performed using a four-point Gauss–Hermite quadrature.

Secondly, the integration over the azimuthal rotations of the monomers is performed. This is made analytic by expanding the vibrational matrix elements in a complete set of functions, which are the same as those used to describe the azimuthal wavefunctions:

$$V_v^{v'}(\phi_A, \phi_B, R) = \sum_{nm} [V_{nm1}^{vv'}(R) \cos n\phi_A \cos m\phi_B + V_{nm2}^{vv'}(R) \cos n\phi_A \sin m\phi_B + V_{nm3}^{vv'}(R) \sin n\phi_A \cos m\phi_B + V_{nm4}^{vv'}(R) \sin n\phi_A \sin m\phi_B]. \quad (17)$$

As only the ν_7 mode of the ethylene monomer is considered explicitly, and this is of symmetry B_{1u}, all the vibrational potential matrix elements $V_v^{v'}(\phi_A, \phi_B, R)$ are of symmetry A_g or B_{1u}. The symmetries of the expansion functions are given in table 1. Thus the expansion simplifies to

$$V_v^{v'}(\phi_A, \phi_B, R) = \sum_{nm} V_{nm1}^{vv'}(R) \cos n\phi_A \cos m\phi_B. \quad (18)$$

Multiplying on the left by $\cos k\phi_A \cos j\phi_B$ and integrating with respect to ϕ_A and ϕ_B gives the expansion coefficients:

$$V_{kj1}^{vv'}(R) = [\pi^2(1+\delta_{0k})(1+\delta_{0j})]^{-1} \int_0^{2\pi} d\phi_A \int_0^{2\pi} d\phi_B \cos k\phi_A \cos j\phi_B V_v^{v'}(\phi_A, \phi_B, R). \quad (19)$$

Since $V_v^{v'}(\phi_A, \phi_B, R)$ of eqn (18) is an even function, this integral needs to be calculated over only half the range of integration and is evaluated using a numerical quadrature with equally spaced points. This expansion converges rapidly; in the present case the coefficients were found to be unimportant for $k, j > 8$.

Numerical Methods

The ethylene normal modes were calculated from a quadratic force field due to Ermer and Lifson.[24] The ν_7 vibration was taken to have its experimental frequency of 949 cm^{-1}, and the rotational energy levels were obtained using rotational constants calculated from Ermer and Lifson's equilibrium geometry. The resulting threshold energies with both monomers in their ground vibrational states are given in table 2. The AVCC–IOS coupled-channel equations were solved using the R-matrix propagator method of Light and Walker,[25,26] with equally spaced (0.02 Å) divisions of the intermolecular distance R from 2.7 to 9.0 Å.

For the calculations in which the monomer wavefunctions have different total symmetries on the two molecules, basis functions corresponding to the ν_7 vibrationally excited state on monomer B were included, but those corresponding to the ν_7 excited

Table 2. Threshold energies for pairs of ethylene molecules in their ground vibrational states (cm^{-1})

k_A/k_B	0	1	2	3	4	5	6	7	8	9	10	11	12	13
0	0.00													
1	3.81	7.62												
2	15.24	19.05	30.48											
3	34.29	38.10	49.53	68.58										
4	60.96	64.77	76.20	95.25	121.92									
5	95.25	99.06	110.49	129.54	156.21	190.50								
6	137.16	140.97	152.40	171.45	198.12	232.41	274.32							
7	186.69	190.50	201.93	220.98	247.65	281.94	323.85	373.38						
8	243.84	247.65	259.08	278.13	304.80	339.09	381.00	430.53	487.68					
9	308.61	312.42	323.85	342.90	369.57	403.86	445.77	495.30	552.45	617.22				
10	381.00	384.81	396.24	415.29	441.96	476.25	518.16	567.69	642.84	689.61	762.00			
11	461.01	464.82	476.25	495.30	521.97	556.26	598.17	647.70	704.85	769.62	842.01	922.02		
12	548.64	552.45	563.88	582.93	609.60	643.85	685.80	735.33	792.48	857.25	929.64	1009.65	1097.28	
13	643.89	647.70	659.13	678.18	704.85	739.14	781.05	830.58	887.73	952.50	1024.89	1104.90	1192.53	1287.78

Table 3. Potential parameters for the potential based on *ab initio* calculations[27] (in atomic units)

	A_{ij}	B_{ij}	C_{ij}	R^0_{ij}
C—C	43.2	1.672	63.6	3.7
C—H	10.2	1.815	9.58	3.4
H—H	2.39	1.956	1.98	2.9
	$q_C = -0.596$	$q_H = 0.218$	$q_0 = 0.320$	

Table 4. Potential parameters for the potential due to Williams[28,29] (in atomic units)

	A_{ij}	B_{ij}	C_{ij}	R^0_{ij}
C—C	98.8	1.905	36.6	3.60
C—H	17.5	1.942	9.29	3.25
H—H	4.19	1.979	2.34	3.10
	$q_C = 0.0$	$q_H = 0.0$	$q_0 = 0.0$	

state on monomer A were not. Calculations using small basis sets indicated that the neglect of basis functions corresponding to the ν_7 excited state on monomer A did not greatly effect the widths of the resonances.

The monomer basis set is formed from products of vibrational and azimuthal rotational functions. This primitive basis set included the seven lowest azimuthal functions of the required symmetry in the ground vibrational state on molecule A and the seven lowest azimuthal functions which give the same total symmetry in each of the ground and the ν_7 vibrationally excited states on molecule B. The basis set used in the scattering calculation is constructed from the primitive basis set by taking products of the functions on the two monomers. All basis functions in which the sum of the azimuthal quantum numbers on the two monomers is greater than 21 were excluded. The size of the resulting basis set depends on the symmetry under consideration, but is typically *ca.* 80 functions.

With the integration parameters and basis sets described above, the calculated predissociation widths are converged to better than ±5%.

Intermolecular Potentials

The intermolecular potential for $C_2H_4+C_2H_4$ is written in the form

$$V_1 = \sum_i \sum_j \left(A_{ij} \exp(-B_{ij}R_{ij}) - \frac{C_{ij}}{R_{ij}^6} \tanh(R_{ij} - R^0_{ij}) + \frac{q_i q_j}{R_{ij}} \right) + \sum_i \frac{q_i q_0}{R_{i0}} + \sum_j \frac{q_0 q_j}{R_{0j}} + \frac{q_0^2}{R} \quad (20)$$

where R_{ij} is the distance from atom i on molecule A to atom j on molecule B, R_{i0} is the distance from atom i on molecule A to the centre of mass of molecule B and R_{0j} is the distance from atom j on molecule B to the centre of mass of molecule A. The ethylene monomers are taken to have a C—C bond length of 1.337 Å, a C—H bond length of 1.103 Å and an H—C—H angle of 117.2°.

Two potentials have been used in the calculations. The first, which is thought to be more accurate and which we have used more extensively, is derived from *ab initio* results;[27] the other is a fit to experimental solid-state data for many different hydrocarbons.[28,29] The parameters A_{ij}, B_{ij}, C_{ij}, R^0_{ij}, q_i, q_j and q_0 used for the two potentials are given in tables 3 and 4, respectively. The differences between predissociation parameters

calculated using the two potentials give an indication of the sensitivity of the results to the intermolecular potential.

The potential based on *ab initio* calculations relies heavily on the results of Wasiutynski *et al.*[27] The short-range parameters A_{ij} and B_{ij} and dispersion coefficients C_{ij} were taken directly from ref. (27). The dispersion term was modified by the inclusion of a hyperbolic tangent damping function[30] as in eqn (20), with the damping parameter R_{ij}^0 taken to be half the distance at the minimum in the atom–atom potential. The electrostatic part of the potential was constructed using a point-charge model, with charges on all the atoms and at the centre of mass of each monomer. The charges were chosen to reproduce the quadrupole moment tensor of the ethylene molecule, as given by an SCF calculation,[31] so that the resulting intermolecular electrostatic potential is accurate in the long range region. In addition, a comparison with interaction energies from a full Distributed Multipole Analysis (DMA)[32] (with multipoles up to $l = 2$ on all atoms) indicates that the electrostatic potential is realistic in the short range region as well. The resulting potential has a minimum at a staggered parallel structure ($\theta_A = \theta_B = 112.3°$, $\phi_A = \phi_B = 47.8°$, $\xi = 0°$); this is close to the structure suggested by various experimental considerations.[33,34] The well depth at the minimum is 428 cm^{-1} and the anisotropy on azimuthal rotation is 302 cm^{-1}. Most of the calculations presented have been carried out using fixed angles ($\theta_A = \theta_B = 112.3°$, $\xi = 0°$).

The potential based on a fit to experimental solid-state data is due to Williams.[28,29] He considered data for n-pentane and n-octane, assuming that the local carbon symmetry was C_{2v}, and fitted intermolecular potential parameters to the observed crystal structures and sublimation energies, assuming a geometric mean combination rule for the attractive coefficients. It should be noted that this potential does not include any electrostatic interaction and hence does not give the correct equilibrium structure for the dimer. The absolute minimum for this potential is found to be at the crossed parallel geometry ($\theta_A = \theta_B = 0°$, $\phi_A = \phi_B = 0°$, $\xi = 90°$). The well depth at the minimum is 329 cm^{-1} and the anisotropy on azimuthal rotation is *ca.* 90 cm^{-1}. Calculations were carried out using the values of the fixed angles $\theta_A = \theta_B = 0°$, $\xi = 90°$. We also considered the geometry $\theta_A = \theta_B = 124°$, $\xi = 0°$, which corresponds more closely to the structure obtained experimentally, although these values of the fixed angles do not correspond to a minimum in this potential.

Such potentials as these are obviously fairly crude, and a high degree of accuracy in the vibrational predissociation widths obtained using them is not expected. However, it is expected that the order of magnitude of the widths will be predicted correctly and that the trends in widths and partial widths will not be sensitive to the more subtle features of the intermolecular potential.

Results and Discussion

We have carried out coupled-channel calculations on the vibrational predissociation of the ethylene dimer. The total widths and corresponding lifetimes for the *ab initio*-based potential[27] are given in table 5. No width is greater than 10^{-5} cm^{-1}; this may be contrasted with early experiments in which a broad line of *ca.* 10 cm^{-1} was observed, but is consistent with the recent work of Snels *et al.*[12] in which structure *ca.* 10^{-4} cm^{-1} wide was resolved.

Widths and lifetimes have also been obtained using the potential due to Williams[28,29] and these are presented in table 6. Although the potential surface used in this case is believed to be less accurate, the difference between the widths calculated using the two potentials should give an indication of their sensitivity to the features of the potential. With the Williams potential, we again find that no width is $>10^{-5}$ cm^{-1}, so that it seems most unlikely that any realistic potential would give widths of the order of 10 cm^{-1}.

The widths presented in table 5 may be contrasted with those calculated for the vibrational predissociation of Ne–C_2H_4.[18] The Ne–C_2H_4 potential well used in the

Table 5. Calculated widths (Γ_m/cm^{-1}), lifetimes (τ_m/s) and resonance energies relative to the ground vibrational state (E_m/cm^{-1}) for six predissociating states of $(C_2H_4)_2$ using the *ab initio* potential[a]

$\theta_A/°$	$\theta_B/°$	$\xi/°$	symmetry	Γ_m/cm^{-1}	τ_m/s	E_m/cm^{-1}
112.3	112.3	0	A_g/B_{2g}	0.66×10^{-7}	8.0×10^{-5}	651.95
112.3	112.3	0	B_{3g}/B_{1g}	0.38×10^{-6}	1.4×10^{-5}	722.56
112.3	112.3	0	B_{1g}/B_{2g}	0.17×10^{-6}	3.1×10^{-5}	651.29
112.3	112.3	0	$A_g/A_g(+)$	0.47×10^{-6}	1.1×10^{-5}	651.23
112.3	112.3	0	$A_g/A_g(-)$	0.23×10^{-6}	2.3×10^{-5}	651.06
140.0	140.0	0	A_g/B_{2g}	0.74×10^{-5}	7.1×10^{-7}	758.10

[a] In the case where two monomers have wavefunctions of the same symmetry, (+) denotes the symmetrised and (−) the antisymmetrised wavefunction.

Table 6. Calculated widths (Γ_m/cm^{-1}), lifetimes (τ_m/s) and resonance energies relative to the ground vibrational state (E_m/cm^{-1}) for two predissociating states of $(C_2H_4)_2$ using the Williams potential[28,29]

$\theta_A/°$	$\theta_B/°$	$\xi/°$	symmetry	Γ_m/cm^{-1}	τ_m/s	E_m/cm^{-1}
0	0	90	B_{2g}/B_{3g}	0.39×10^{-6}	1.4×10^{-5}	693.45
124	124	0	B_{2g}/B_{3g}	0.99×10^{-5}	5.3×10^{-7}	797.64

Table 7. Partial widths ($\Gamma_{mk_Ak_B}/10^{-9}\,cm^{-1}$) for the resonances of symmetry A_g/B_{2g} and B_{3g}/B_{1g} at the fixed angles ($\theta_A=\theta_B=112.3°$, $\xi=0°$) using the *ab initio*-based potential[27]

	k_B						
k_A	1	3	5	7	9	11	13
				A_g/B_{2g}			
0	0.08	0.51	2.3	3.1	1.4	0.08	2.9
2	0.31	0.40	1.1	1.9	1.1	3.0	
4	0.39	1.1	0.26	0.31	1.6	2.5	
6	0.32	0.73	0.4	0.06	2.4	8.8	
8	0.73	1.0	0.76	1.1	0.56		
10	1.7	2.0	0.96	2.5			
12	6.1	6.3	5.4				
				B_{3g}/B_{1g}			
2	2.2	2.6	3.1	1.2	3.1	4.0	80.0
4	7.0	1.6	1.6	4.6	18.0	27.0	19.0
6	11.0	0.41	0.32	0.83	7.7	33.0	
8	27.0	4.2	3.0	3.7	3.5	14.0	
10	29.0	9.6	6.3	16.0	2.1		
12	15.0	12.0	9.8				

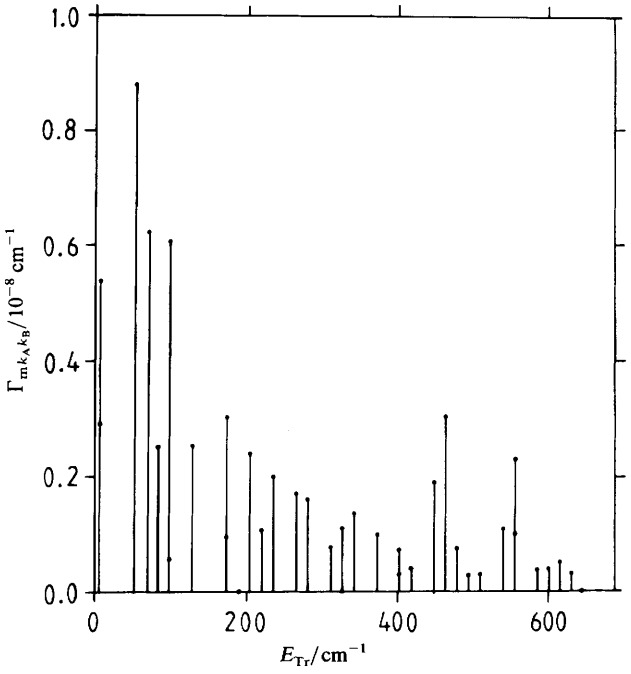

Fig. 2. Plot of partial width, $\Gamma_{mk_Ak_B}$, against relative translational energy of the products, E_{Tr}, for predissociation of the lowest $v_7 = 1$ excited state of symmetry A_g/B_{2g}.

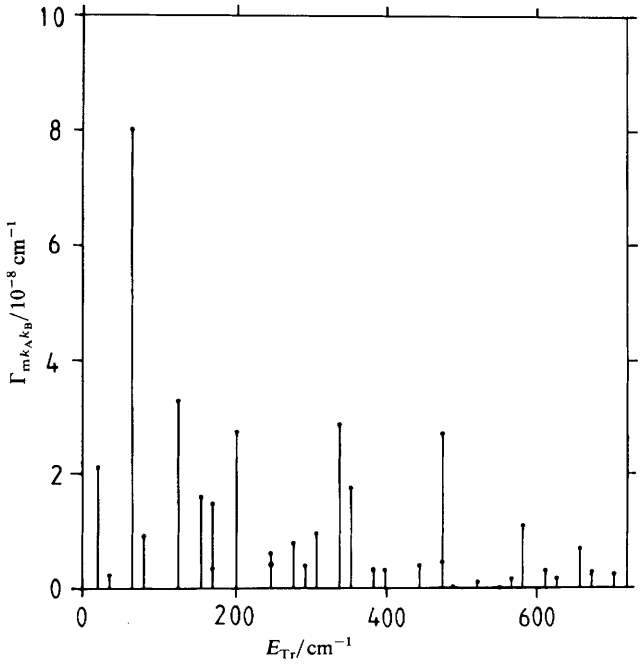

Fig. 3. Plot of partial width, $\Gamma_{mk_Ak_B}$, against relative translational energy of the products, E_{Tr}, for predissociation of the lowest $v_7 = 1$ excited state of symmetry B_{3g}/B_{1g}.

calculation was very shallow (113 cm^{-1}), allowing predissociation to occur to give ethylene in its ν_{10} vibrationally excited state. Such vibration–vibration transfer is much more efficient than vibration–rotation transfer, and widths of the order of 10^{-2} cm^{-1} were obtained in the computations. The ν_{10} vibrationally excited channel of C_2H_4 is energetically inaccessible for the predissociation of the ethylene dimer, which has a much deeper well, so that the dimer is much longer lived.

Partial widths calculated for two of the resonances using the *ab initio*-based potential are presented in table 7. Plots of the partial widths as a function of the relative translational energy of the products are given in fig. 2 and 3. For both resonances there is a significant increase in the partial widths as the energy gap between the predissociating state and the product states becomes small, so that the average relative translational energy of the products is small compared with the total energy available. This is consistent with previous coupled-channel calculations on atom–diatomic molecule systems.[15]

Approximate Methods for Calculating Linewidths

Ewing[35] has suggested that a curve-crossing mechanism might account for lifetimes of the ethylene dimer on a picosecond timescale. We have investigated this mechanism and carried out calculations to determine the magnitude of its effect.

When the ethylene monomers have little rotational energy, their orientations are localised near the equilibrium geometry of the complex. Since this is a staggered parallel structure, the hydrogen atoms do not come into close contact and the equilibrium intermolecular distance is relatively small. Conversely, when the ethylene monomers have large amounts of energy associated with rotation about their C—C axes, no such localisation is possible and the equilibrium intermolecular distance is much larger. Ewing[35] suggested that such an effect would produce a curve-crossing between low rotational levels of the upper vibrational state and highly excitated rotational levels of the ground vibrational state, and that such a curve crossing might lead to predissociation lifetimes of the order of 10^{-10} s.

To test the plausibility of this mechanism, we have examined effective potentials constructed by diagonalising the ground-state and upper vibrational state potential matrices of eqn (13) at several values of the intermolecular distance R, then drawing curves through eigenvalues corresponding to a smooth variation in the eigenvectors. Representative effective potentials calculated using the set of fixed angles $(\theta_A, \theta_B, \xi) = (112.3°, 112.3°, 0°)$ are shown in fig. 4(a). Curve-crossings do indeed occur, but only for large amounts of rotational excitation in the ground vibrational state. However, the amount of rotational excitation required to produce a curve-crossing is smaller when the repulsive wall anisotropy is greater. This is shown by the effective potentials of fig. 4(b), which were calculated using the fixed angles (140°, 140°, 0°), for which the wall anisotropy is a maximum. It can be seen that in fig. 4(b) there are favourable curve-crossings for lower values of the azimuthal rotational energy.

We have estimated the lifetime of the complex due to these curve-crossings by using a simple Landau–Zener model.[35,36] In this approximation, the rate of crossing from one curve to the other is

$$\tau^{-1} = \nu P_{lu} \tag{21}$$

where ν is the frequency with which the crossing point is passed and P_{lu} is the probability of passing from the upper to the lower curve. If the crossing point lies within the classically allowed region, ν is the zero point oscillation frequency of the van der Waals bond. The transition probability is then given by

$$P_{lu} = \left(\frac{2\pi}{\hbar v_c}\right) \frac{|V_{lu}(R_c)|^2}{|S_l - S_u|}, \tag{22}$$

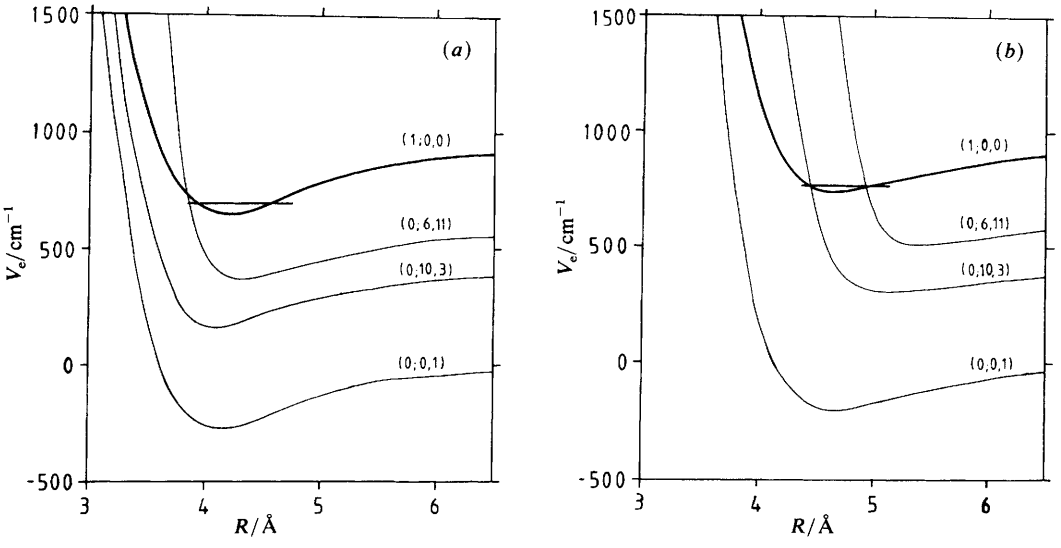

Fig. 4. Effective potentials curves of $(C_2H_4)_2$ at fixed angles (*a*) $\theta_A = \theta_B = 112.3°$, $\xi = 0$ and (*b*) $\theta_A = \theta_B = 140.0°$, $\xi = 0°$. The curves are labelled in the manner $(v_7; k_A, k_B)$.

where v_c is the velocity of motion along R at the crossing point (R_c), and is given by $\frac{1}{2}\mu v_c^2 = W_0$, where W_0 is the zero-point energy of the van der Waals bond. The quantities S_u and S_l are the slopes of the upper and lower effective potentials at the curve crossing and $V_{lu}(R_c)$ is the potential matrix element between the upper and lower effective potentials at the crossing point R_c.

The probability for crossing from one curve to another is greatest if the slopes of the upper and lower curves are similar and the matrix element $|V_{lu}|$ is large. For the crossing point to be reached during every zero-point oscillation it must be in the classically allowed region and so the optimum curve crossing will be of the form of the effective potential labelled (0; 10, 3) in fig. 4(*b*). For this crossing, the slopes of the upper and lower curves are 280 cm^{-1} Å^{-1} and 2300 cm^{-1} Å^{-1}, respectively, while the matrix element $|V_{lu}|$ is 0.012 cm^{-1}. For a zero-point energy of 25 cm^{-1}, this gives a lifetime of 3×10^{-5} s, corresponding to a partial width of 2×10^{-7} cm^{-1}. We have also carried out the full AVCC-IOS calculation for these values of the fixed angles, and obtain $\Gamma_m = 0.99 \times 10^{-5}$ cm^{-1}, with a largest partial width of 9.2×10^{-7} cm^{-1}, in quite good agreement with the Landau-Zener prediction. Thus predissociation by the curve-crossing mechanism can occur, but is not nearly as fast as suggested previously.[35]

The Landau-Zener analysis explains three otherwise puzzling phenomena apparent in the AVCC-IOS calculations. First, the total width at the set of fixed angles (112.3°, 112.3°, 0°), which correspond to the equilibrium geometry, is more than an order of magnitude less than the width found at the set of fixed angles (140°, 140°, 0°). This is because at the latter set of fixed angles the hydrogen atoms come into close contact on azimuthal rotation, giving a large repulsive wall anisotropy and a favourable crossing. This does not occur for the set of fixed angles (112.3°, 112.3°, 0°), where curve crossings occur only for very highly rotationally excited states which have small coupling elements $|V_{lu}(R_c)|$ with the predissociating state.

Secondly, it was found in the coupled-channel calculations that the calculated level widths decreased dramatically as the size of the rotational basis set increased. This arises because the addition of extra rotational basis functions decreases the energies of the effective potentials below them, so that favourable curve crossings occur only for

effective potentials corresponding to larger azimuthal quantum numbers; the corresponding coupling elements $|V_{lu}(R_c)|$ are much smaller, and lead to much smaller level widths.

Thirdly, for the AVCC-IOS calculation at fixed angles (140°, 140°, 0°), the channels which have little kinetic energy release have very small partial widths; this is not as expected from momentum gap arguments. In the Landau–Zener picture, these channels correspond to effective potentials outside the one labelled (0; 6, 11) in fig. 4(*b*) and have curve crossings at large values of the intermolecular distance R_c, outside the region sampled by the zero-point stretching motion. In addition, the coupling elements $|V_{lu}(R_c)|$ are very small in this region. The combination of these two factors makes such curve crossings unfavourable and leads to small partial widths.

Conclusions

We have extended the AVCC-IOS approximation to symmetric top–symmetric top systems and applied the method to the vibrational predissociation of the ethylene dimer. We have calculated level energies, widths and product state distributions for predissociation of complexes containing ethylene in the ν_7 excited state. The calculations were carried out at fixed angles θ_A, θ_B and ξ; for the values corresponding to the equilibrium geometry the predissociation widths were found to be *ca.* 10^{-6} cm^{-1}, corresponding to lifetimes of *ca.* 10^{-6} s.

Apart from the approximation of carrying out the calculation with three of the five orientation angles fixed, the ethylene molecule was approximated as a symmetric top and anharmonicity and coriolis coupling effects in the ethylene monomer were neglected. However, it seems very unlikely that any of these approximations could cause drastic errors in the predissociation widths. Linewidths calculated using a different intermolecular potential are also *ca.* 10^{-6} cm^{-1} and so it appears that errors due to inaccuracies in the potential do not cause large errors in the widths. It thus seems unlikely that the broad spectra observed in early experiments on this system were homogeneously broadened, and our results support the observation of Snels *et al.*[12] that fine structure exists within the broad envelopes.

We calculated product state distributions for the predissociation, and found that these indicated a preference for the complex to dissociate to produce rotationally excited ethylene; an average energy release of *ca.* 200 cm^{-1} was predicted. We also investigated a curve-crossing mechanism previously discussed by Ewing and found that the mechanism could occur, but that it did not greatly enhance the predissociation widths. The curve-crossing mechanism is in any case fully accounted for by AVCC-IOS calculations. Therefore, it is very unlikely that such a mechanism can account for picosecond lifetimes.

Despite the extensive experimental work which has been carried out on the vibrational predissociation of the ethylene dimer, there is still much to be learnt about its spectrum. High quality theoretical calculations will be a valuable aid to the interpretation of the spectroscopic data and eventually it may be possible to calculate a full photodissociation spectrum of the ethylene dimer.

The calculations were carried out on the CRAY-1S computer of the University of London Computer Centre. This work was supported by the S.E.R.C.

References

1 K. C. Janda, *Adv. Chem. Phys.*, 1985, **60**, 201.
2 G. Fischer, R. E. Miller, P. F. Vohralik and R. O. Watts, *J. Chem. Phys.*, 1985, **83**, 1471.
3 R. E. Miller and R. O. Watts, *Chem. Phys. Lett.*, 1984, **105**, 409.
4 A. S. Pine, W. J. Lafferty and B. J. Howard, *J. Chem. Phys.*, 1984, **81**, 2939.
5 C. M. Western, M. P. Casassa and K. C. Janda, *J. Chem. Phys.*, 1984, **80**, 4781.
6 M. P. Casassa, D. S. Bomse and K. C. Janda, *J. Chem. Phys.*, 1981, **74**, 5044.

7 M. A. Hoffbauer, K. Liu, C. F. Giese and W. R. Gentry, *J. Chem. Phys.*, 1983, **78**, 5567.
8 W. L. Liu, K. Kolenbrander and J. M. Lisy, *Chem. Phys. Lett.*, 1984, **112**, 585.
9 A. Mitchell, M. J. McAuliffe, C. F. Giese and W. R. Gentry, *J. Chem. Phys.*, 1985, **83**, 4271.
10 F. Huisken, H. Meyer, C. Lauenstein, R. Sroka and U. Buck, *J. Chem. Phys.*, 1986, **84**, 1042.
11 U. Buck, personal communication.
12 M. Snels, R. Fantoni, M. Zen, S. Stolte and J. Reuss, *Chem. Phys. Lett.*, 1986, **124**, 1.
13 E. Segev and M. Shapiro, *J. Chem. Phys.*, 1983, **78**, 4969.
14 J. M. Hutson, C. J. Ashton and R. J. Le Roy, *J. Phys. Chem.*, 1983, **87**, 2713.
15 J. M. Hutson, *J. Chem. Phys.*, 1984, **81**, 2357.
16 I. F. Kidd and G. G. Balint-Kurti, *J. Chem. Phys.*, 1985, **82**, 93.
17 N. Halberstadt, Ph. Bréchignac, J. A. Beswick and M. Shapiro, *J. Chem. Phys.*, 1986, **84**, 170.
18 J. M. Hutson, D. C. Clary and J. A. Beswick, *J. Chem. Phys.*, 1984, **81**, 4474.
19 D. C. Clary, *J. Chem. Phys.*, 1984, **81**, 4466.
20 G. Herzberg, *Infrared and Raman Spectra of Polyatomic Molecules* (Van Nostrand, New York, 1945).
21 R. T. Pack, *J. Chem. Phys.*, 1974, **60**, 633.
22 H. Goldstein, *Classical Mechanics* (Addison-Wesley, Reading, 1950).
23 C. J. Ashton, M. S. Child and J. M. Hutson, *J. Chem. Phys.*, 1983, **78**, 4025.
24 O. Ermer and S. Lifson, *J. Am. Chem. Soc.*, 1973, **95**, 4121.
25 J. C. Light and R. B. Walker, *J. Chem. Phys.*, 1976, **65**, 4272.
26 E. B. Stechel, R. B. Walker and J. C. Light, *J. Chem. Phys.*, 1978, **69**, 3518.
27 T. Wasiutynski, A. van der Avoird and R. M. Berns, *J. Chem. Phys.*, 1978, **69**, 5288.
28 D. E. Williams, *J. Chem. Phys.*, 1966, **45**, 3770.
29 D. E. Williams, *J. Chem. Phys.*, 1967, **47**, 4680.
30 P. Huxley, D. B. Knowles, J. N. Murrell and J. D. Watts, *J. Chem. Soc., Faraday Trans. 2*, 1984, **80**, 1349.
31 P. W. Fowler, personal communication.
32 A. J. Stone and M. Alderton, *Mol. Phys.*, 1985, **56**, 1047.
33 G. J. H. van Nes and A. Vos, *Acta Crystallogr., Sect. B*, 1977, **33**, 1653.
34 E. Rytter and G. M. Gruen, *Spectrochim. Acta, Part A*, 1979, **35**, 199.
35 G. E. Ewing, *Chem. Phys.*, 1981, **63**, 411; *Faraday Discuss. Chem. Soc.*, 1982, **73**, 325.
36 L. D. Landau and E. M. Lifshitz, *Quantum Mechanics* (Pergamon, Oxford, 1977).

Received 18*th May*, 1986